Supplementary Information

Negative induction effect of "graphite" N on graphene quantum dots: tunable band gap photoluminescence

Chong Zhu [a b c †], Siwei Yang [c †], Gang Wang [c], Runwei Mo [c], Peng He [c], Jing Sun [c], Zengfeng Di [c], Ningyi Yuan [a b], Jianning Ding [a b*], Guqiao Ding [c *], Xiaoming Xie [c]

[a] School of Materials Science and Engineering, Jiangsu Collaborative Innovation Center for Photovolatic Science and Engineering, Changzhou University, Changzhou, 213164, Jiangsu, China

[b] Jiangsu Province Cultivation base for State Key Laboratory of Photovoltaic Science and Technology, Changzhou University, Changzhou, 213164, Jiangsu, China.

[c] State Key Laboratory of Functional Materials for Informatics, Shanghai Institute of Microsystem and Information Technology, Chinese Academy of Science, Shanghai, 200500, China.

† These authors (Chong Zhu and Siwei Yang) contributed equally.

* Corresponding author: Prof. Jianning Ding, dingjn@cczu.edu.cn,

Prof. Guqiao Ding, gqding@mail.sim.ac.cn.

Experimental Section

Materials

Melamine (99.5 %), RhB (99.5 %), NaCl (99.5 %), KCl (99.5 %), $MgCl_2$ (99.5 %), $CaCl_2$ (99.5 %), $ZnCl_2$ (99.5 %), $CuCl_2$ (99.5 %), $FeCl_3$ (99.5 %), $NaNO_3$ (99.5 %), Na_2CO_3 (99.5 %), Na_2SO_4 (99.5 %), HCl (30 wt. %) and NaOH (99.5 %) were purchased from Aladdin (Shanghai, China) and used as received without further purification. Graphene oxide were purchased from SIBAT (Shanghai, China) and used as received without further purification. The water used throughout all experiments was purified through a Millipore system.

Synthesis of N-GQDs

The preparation process of N-GQDs was run on the piston-cylinder apparatus (RTK-PC1, ROCKTEK, Hubei, China) with solid confining media. The diameter of pressure chamber is 9.0 mm. Typically, melamine powder was put into home-made platinum tube. The pressure was gradually increased to 4.0 GPa, then the melamine were heated for 72 h under 1000 ^oC. The heating and freezing rates are 100 $^oC\ h^{-1}$. The pressure and release rate are 0.2 GPa h^{-1}. After the reaction, the grey black powder was obtained and the yield is ~63 wt. %.

Characterization

TEM measurements were carried out on a spherical aberration-corrected TEM (FEI Titan 80-300) at 80 kV. AFM topography were carried out on Bruker Dimension Icon AFM microscope. X-ray photoelectron spectra (XPS) were carried out on a PHI Quantera II system (Ulvac-PHI, INC, Japan). The UV-vis spectra were obtained on a UV5800 Spectrophotometer. PL and PLE spectra were recorded on a PerkinElmer LS55 luminescence spectrometer (PerkinElmer Instruments, U.K.) at room temperature in aqueous solution. The stability of these products was determined via contrast the fluorescent emission intensity of products aqueous solution under different conservative time at room temperature.

The quantum yield (φ) of GQDs was calculated according to equation 1:[s1]

$$\varphi = \varphi_R \times \frac{I}{I_R} \times \frac{A_R}{A} \times \frac{\eta^2}{\eta_R^2} \quad (1)$$

where I is the measured integrated emission intensity, η is the refractive index of the solvent, A is the optical density, and the subscript R refers to the reference standard with a known φ (RhB in ethanol solution, φ_R=0.68). The absorbance was kept under 0.1 at excitation wavelength.

Supplementary figures and tables

Fig. S1 Digital photo of precursor

Fig. S2 Digital photo of N-GQDs.

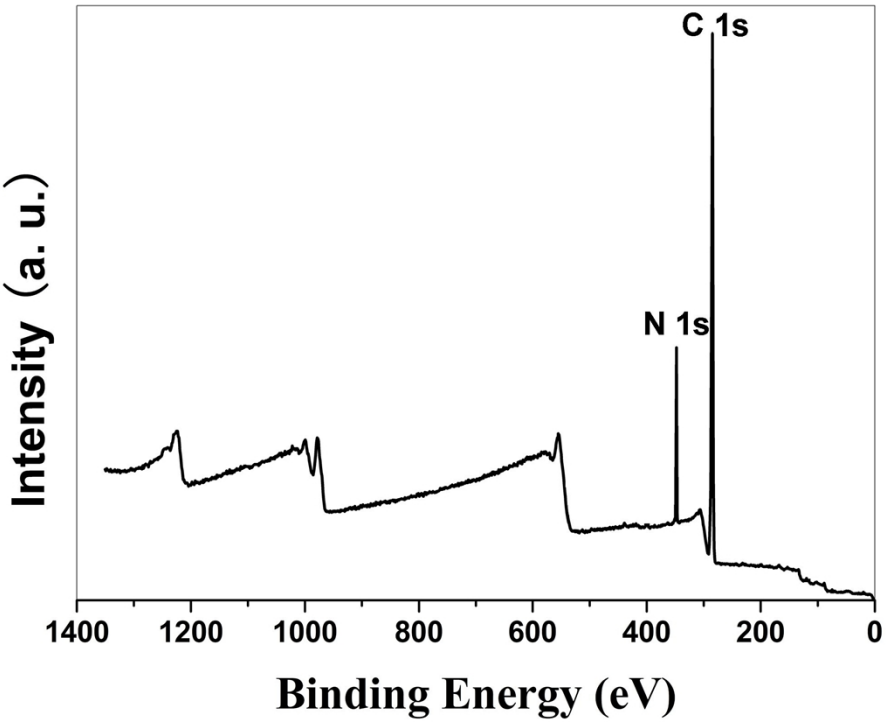

Fig. S3 XPS spectrum of N-GQDs.

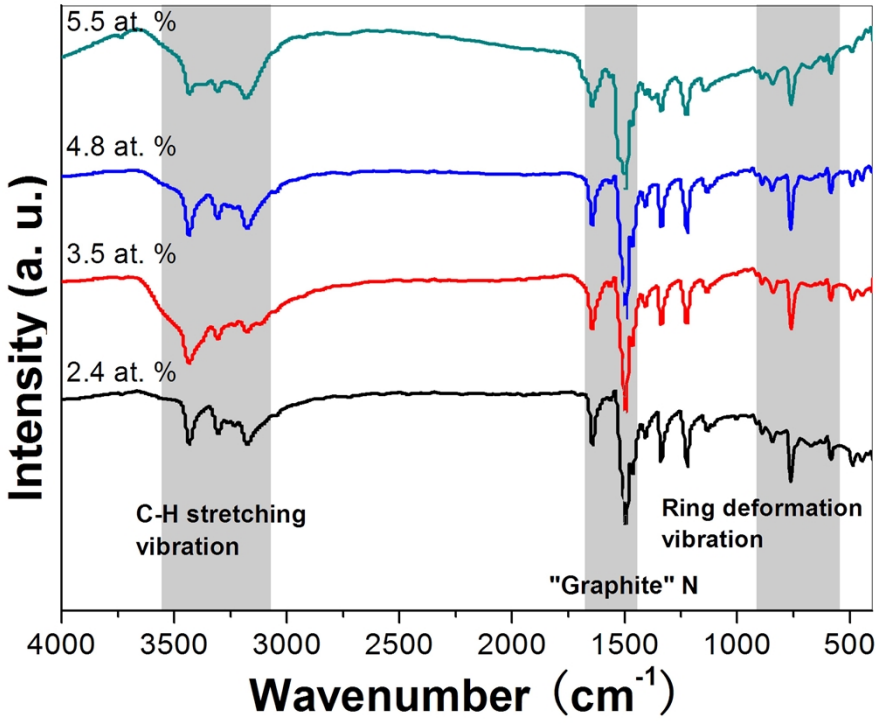

Fig. S4 FT-IR spectra of N-GQDs with doping concentrations.

Table S1 A brief summary of XPS results of N-GQDs with different doping concentration.

Reaction temperature (°C)	C 1s						N 1s		Doping concentration (at. %)
	C-C/C=C (eV)	Ratio (%)	C=N (eV)	Ratio (%)	C-N (eV)	Ratio (%)	"graphitic" N (eV)	Ratio (%)	
800	284.8	68	286.8	25	287.6	7	400.3	100	6.4
900	284.9	74	286.8	20	287.9	6	400.1	100	5.5
1000	284.8	79	286.9	17	287.8	4	400.2	100	4.8
1100	284.6	84	287.2	13	287.7	3	400.2	100	3.5
1200	284.7	91	286.8	7	287.6	2	400.1	100	2.4

Table S2 A brief summary of elemental analysis results of N-GQDs with different doping concentration.

Reaction temperature (°C)	Doping concentration (at. %) [a]	Doping concentration (at. %) [b]
800	6.3	6.4
900	5.4	5.5
1000	5.0	4.8
1100	3.4	3.5
1200	2.6	2.4

[a] **obtained by elemental analysis results**

[b] **obtained by XPS results**

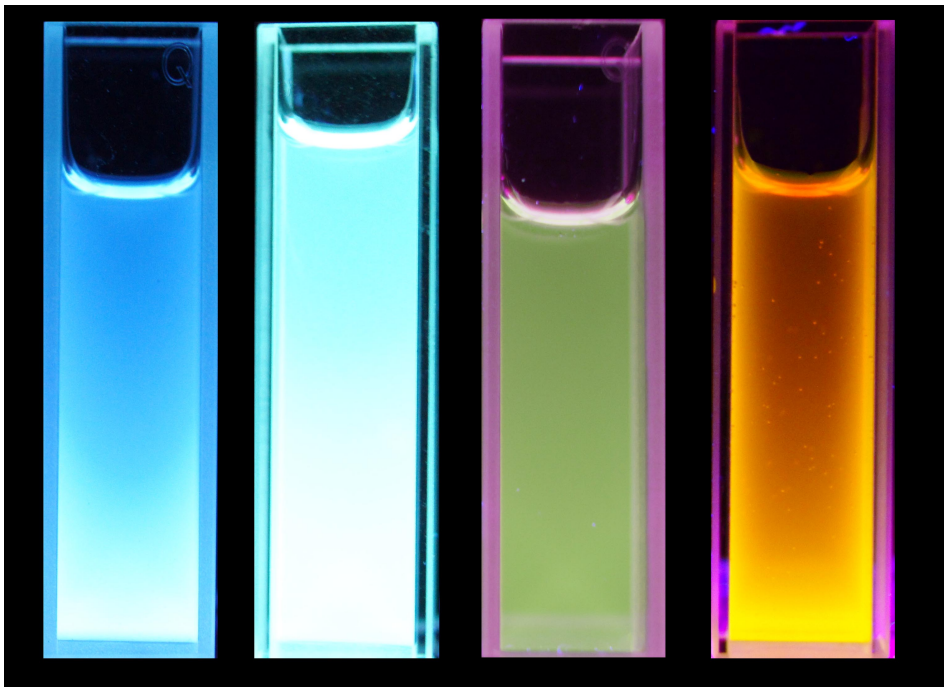

Fig. S5 Digital photo of N-GQDs aqueous solutions (doping concentration: 5.5, 4.8, 3.5 and 2.4 at. %

from left to right) under 365 nm UV light.

Table S3 A brief summary of optical properties of N-GQDs with different doping concentration.

Reaction temperature (°C)	Doping concentration (at. %)	Uv-vis				PL		
		E_g (eV)	π-π* transition (nm)	n-π* transition (nm)	Band-gap transition (nm)	λ_{ex} (nm)	λ_{em} (nm)	φ (%)
800	6.4	5.11	211	232	247	268	344	83
900	5.5	3.79	210	240	270	295	402	84
1000	4.8	3.45	243	264	341	362	436	79
1100	3.5	2.91	277	282	412	431	495	76
1200	2.4	2.38	295	314	524	544	587	72

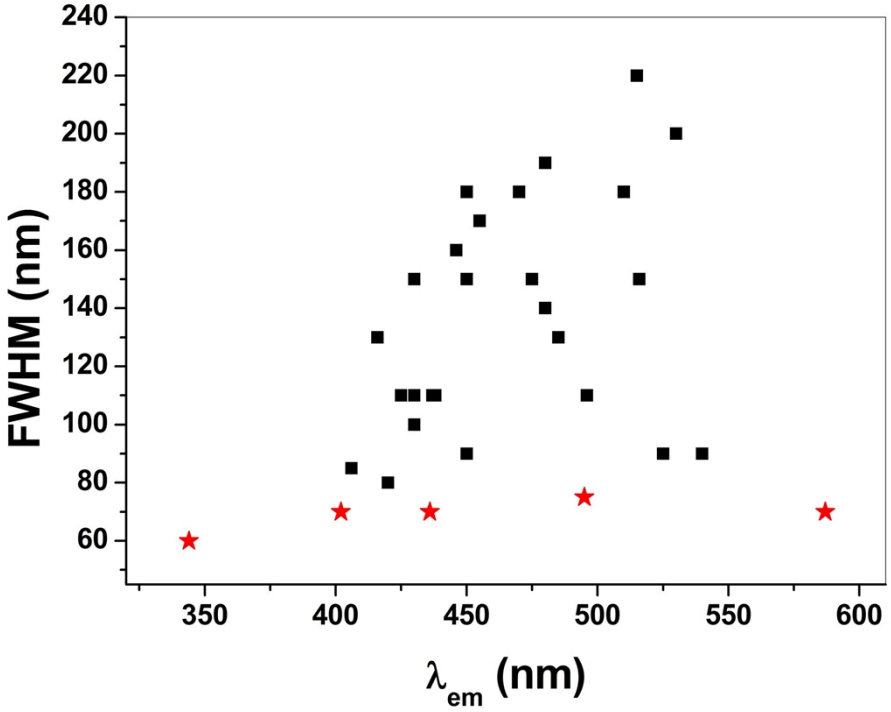

Fig. S6 A brief summary of λ_{em} and its full width at half maximum (FWHM) of N-GQDs with different doping concentration (red five-pointed star) and previously reported GQDs (black squares). [2-17]

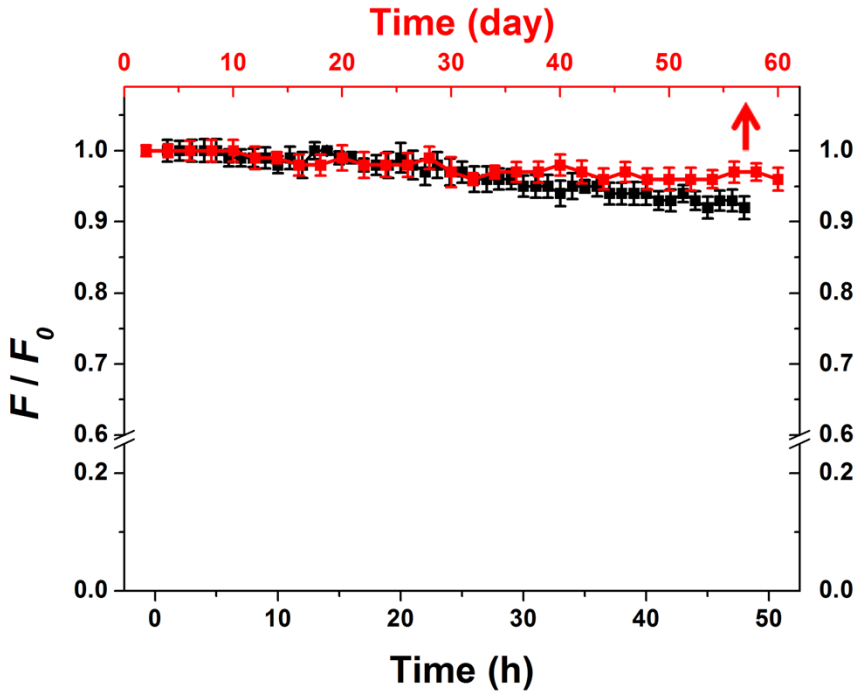

Fig. S7 The stability N-GQDs under UV light (black curve) and visible light (red curve) at room temperature. The F and F_0 are PL intensity of N-GQDs (doping concentration: 4.8 at. %) when t=0 and at corresponding times, respectively.

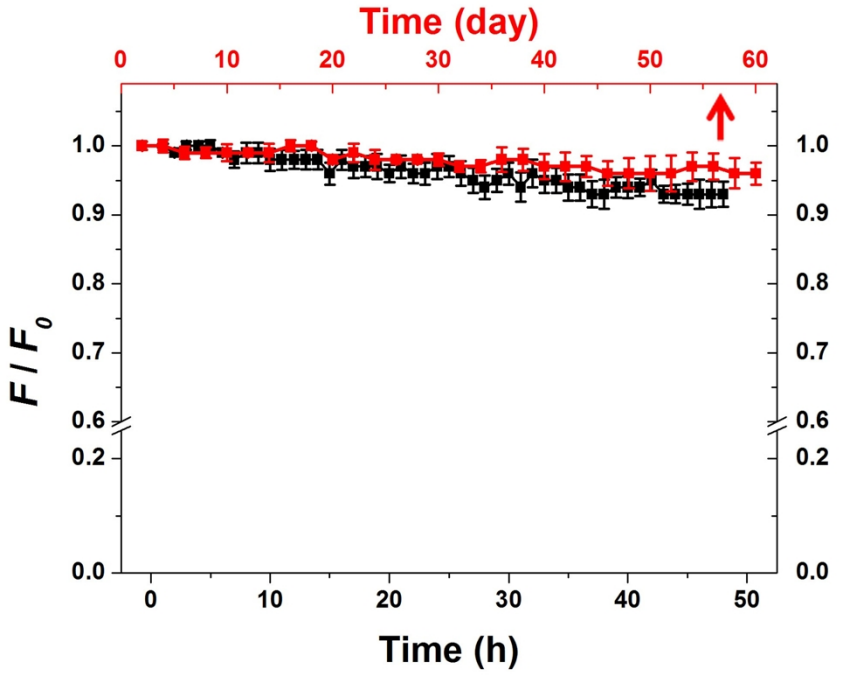

Fig. S8 The stability N-GQDs under UV light (black curve) and visible light (red curve) at room temperature. The F and F_0 are PL intensity of N-GQDs (doping concentration: 3.5 at. %) when t=0 and at corresponding times, respectively.

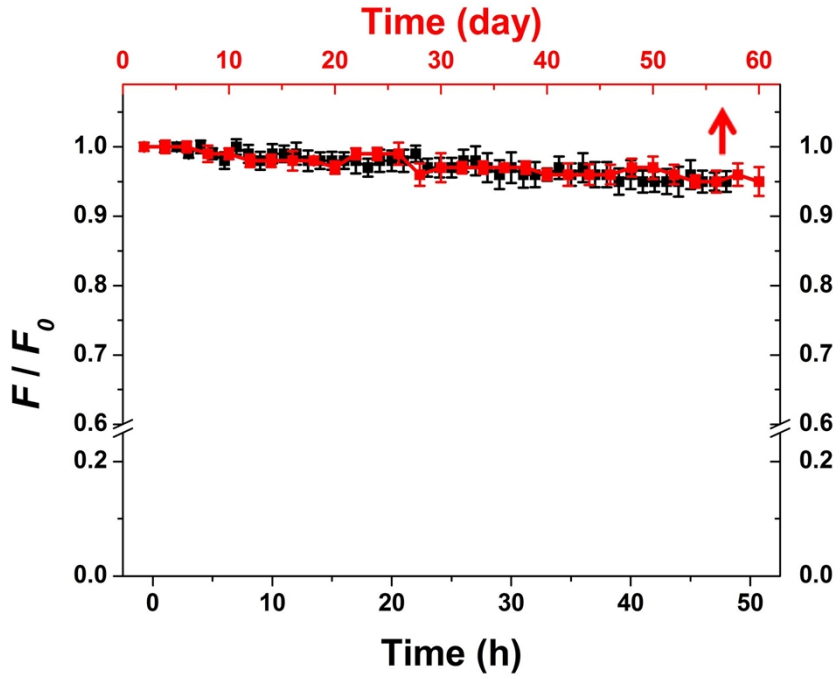

Fig. S9 The stability N-GQDs under UV light (black curve) and visible light (red curve) at room temperature. The F and F_0 are PL intensity of N-GQDs (doping concentration: 2.4 at. %) when t=0 and at corresponding times, respectively.

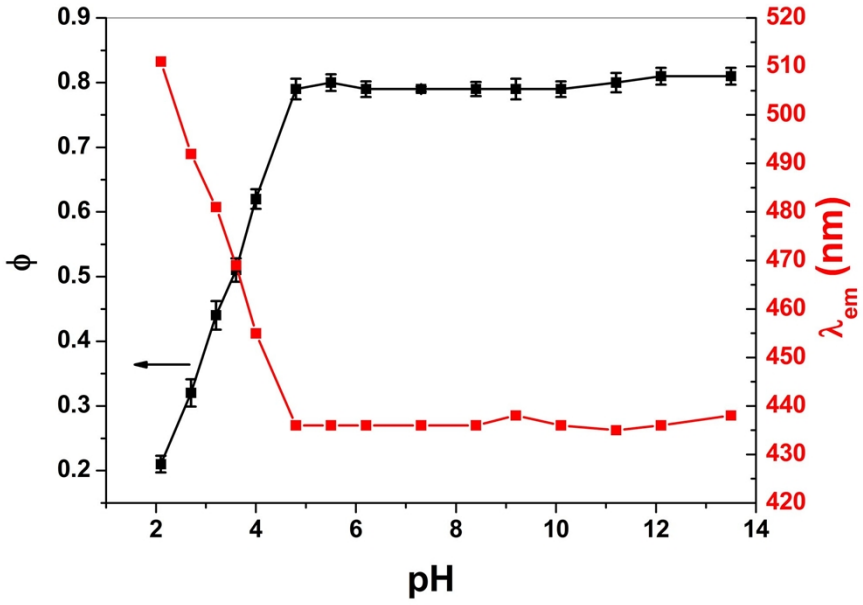

Fig. S10 λ_{em} (black curve) and φ (red curve) of N-GQDs (doping concentration: 4.8 at.%) under different pH.

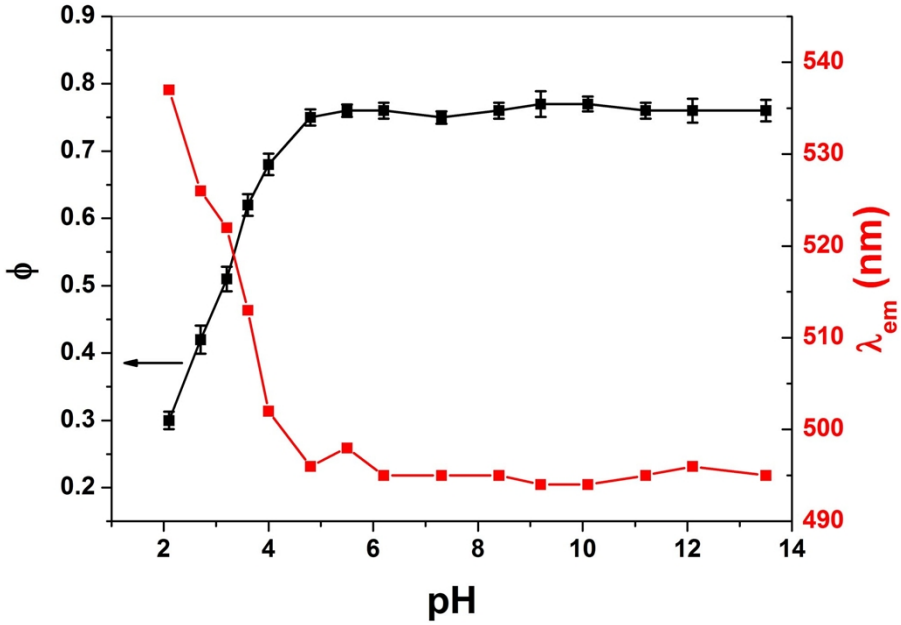

Fig. S11 λ_{em} (black curve) and φ (red curve) of N-GQDs (doping concentration: 3.5 at.%) under different pH.

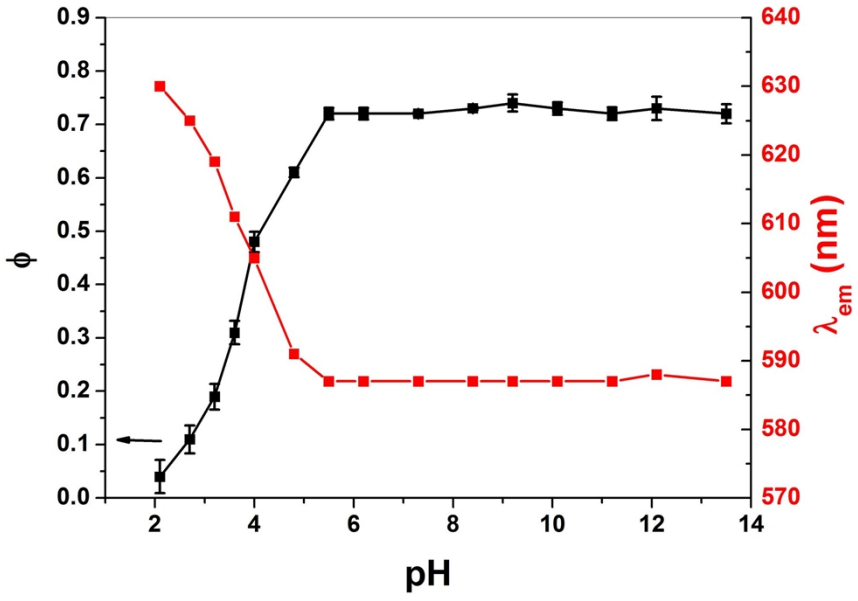

Fig. S12 λ_{em} (black curve) and φ (red curve) of N-GQDs (doping concentration: 2.4 at.%) under different pH.

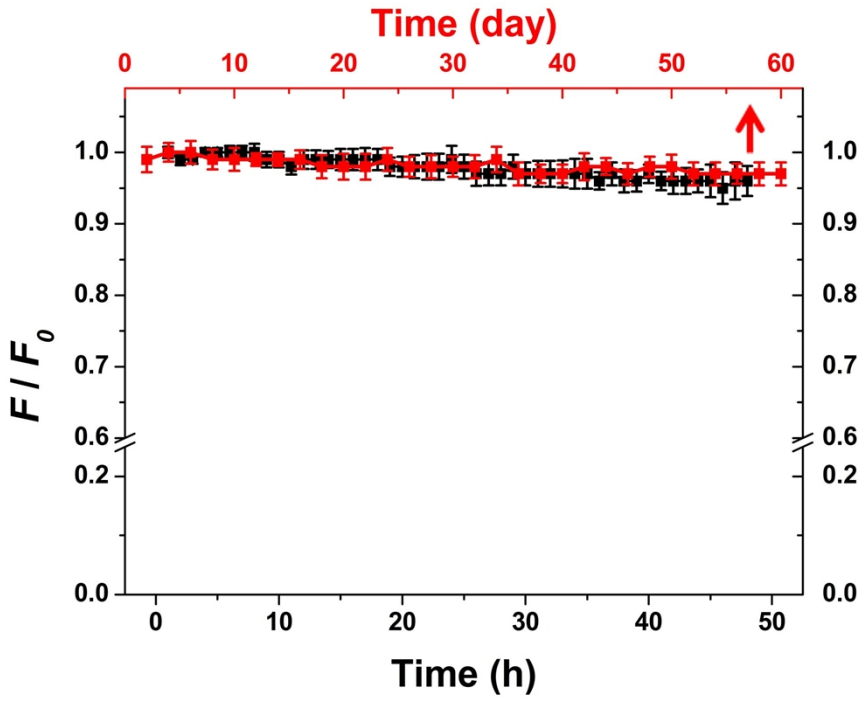

Fig. S13 The stability N-GQDs under UV light (black curve) and visible light (red curve) at room temperature. The F and F_0 are PL intensity of N-GQDs (doping concentration: 6.4 at. %) when t=0 and at corresponding times, respectively.

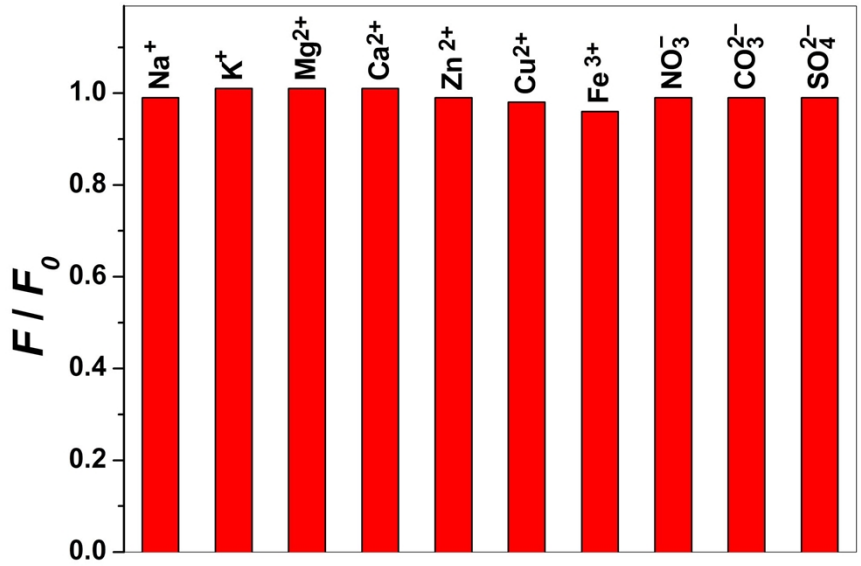

Fig. S14 The difference in PL intensity of N-GQD aqueous solution between the blank and solutions containing different common positive ions and negative ions (F_0 and F are PL intensities in the absence and presence of ions, respectively. The concentrations of all ions are all 0.1 M, the concentrations of N-GQD is 0.5 mg mL^{-1}).

References

[S1] J. D. Demas and G. A Crosby, *J. Phys. Chem.*, 1971, **75**, 991. X. H. Zhu, X. Xiao, X. X. Zuo, Y. Liang and J. M. Nan, *Part. Part. Syst. Charact.*, 2014, **31**, 801.

[S2] Y. Q. Dai, H. Long, X. T. Wang, Y. M. Wang, Q. Gu, W. Jiang, Y. C. Wang, C. C. Li, T. Y. Helen Zeng, Y. M. Sun and J. Zeng, *Part. Part. Syst. Charact.*, 2014, **31**, 597.

[S3] D. Qu, M. Zheng, P. Du, Y. Zhou, L. G. Zhang, D. Li, H. Q. Tan, Z. Zhao, Z. G. Xie and Z. C. Sun, *Nanoscale*, 2013, **5**, 12272.

[S4] M. B. Wu, Y. Wang, W. T. Wu, C. Hu, X. N. Wang, J. T. Zheng, Z. T. Li, B. Jiang and J. S. Qiu, *Carbon*, 2014, **78**, 480.

[S5] Z. L. Wu, M. X. Gao, T. T. Wang, X. Y. Wan, L. L. Zheng and C. Z. Huang, *Nanoscale*, 2014, **6**, 3868.

[S6] Q. Lu, W. Wei, Z. X. Zhou, Z. X. Zhou, Y. J. Zhang and S. Q. Liu, *Analyst*, 2014, **139**, 2404.

[S7] L. Wang, S. J. Zhu, H. Y. Wang, S. N. Qu, Y. L. Zhang, J. H. Zhang, Q. D. Chen, H. L. Xu, W. Han, B. Yang and H. B. Sun, *ACS Nano*, 2014, **8**, 2541.

[S8] D. Niedzialek, V. Lemaur, D. Dudenko, J. Shu, M. R. Hansen, J. W. Andreasen, W. Pisula, K. Müllen, J. Cornil and D. Beljonne, *Adv. Mater.*, 2013, **25**, 1939.

[S9] Q. Liu, B. D. Guo, Z. Y. Rao, B. H. Zhang and J. R. Gong, *Nano Lett.*, 2013, **13**, 2436.

[S10] H. J. Sun, N. Gao, L. Wu, J. S. Ren, W. L. Wei and X. G. Qu, *Chem. Eur. J.*, 2013, **19**, 13362.

[S11] R. Q. Ye, C. S. Xiang, J. Lin, Z. W. Peng, K. W. Huang, Z. Yan, P. C. Nathan, L. G. Erro Samuel, C. C. Hwang, G. D. Ruan, G. Ceriotti, A. R. O. Raji, A. A. Martĺ and M. T. James, *Nat. Commun.*, 2013, **4**, 2943.

[S12] X. Wu, F. Tian, W. X. Wang, J. Chen, M. Wu and X. J. Zhao, *J. Mater. Chem. C*, 2013, **1**, 4676.

[S13] L. B. Tang, R. B. Ji, X. M. Li, G. X. Bai, C. P. Liu, J. H. Hao, J. Y. Lin, H. X. Jiang, K. S. Teng, Z. B. Yang and S. P. Lau, *ACS Nano*, 2014, **8**, 6312.